

Article

Direct Laser Interference Patterning of Diffraction Gratings in Safrofilcon-A Hydrogel: Fabrication and Hydration Assessment

Daniel Sola ^{1,2,*} , Stephan Milles ¹ and Andrés F. Lasagni ^{1,3}

¹ Institut für Fertigungstechnik, Technische Universität Dresden, 01069 Dresden, Germany; stephan.milles@tu-dresden.de (S.M.); andres_fabian.lasagni@tu-dresden.de (A.F.L.)

² Laboratorio de Óptica, Centro de Investigación en Óptica y Nanofísica, Campus Espinardo, Universidad de Murcia, 30100 Murcia, Spain

³ Fraunhofer Institut für Werkstoff- und Strahltechnik IWS, Winterbergstr. 28, 01277 Dresden, Germany

* Correspondence: daniel.sola@tu-dresden.de

Abstract: Refractive index modification by laser micro-structuring of diffractive optical devices in ophthalmic polymers has recently been applied for refractive correction in the fields of optics and ophthalmology. In this work, Safrofilcon-A hydrogel, used as soft contact lenses, was processed by direct laser interference patterning (DLIP) to fabricate linear periodic patterns on the surface of the samples. Periodic modulation of the surface was attained under two-beam interference by using a Q-switched laser source with emission at 263 nm and 4 ns pulse duration. Features of processed areas were studied as a function of both the interference spatial period and the laser fluence. Optical confocal microscopy used to evaluate the topography of the processed samples showed that both structured height and surface roughness increased with laser fluence. Static water contact angle (WCA) measurements were carried out with deionized water droplets on the structured areas to evaluate the hydration properties of DLIP structures. It was observed that the laser structured areas induced a delay in the hydration process. Finally, microstructural changes induced in the structured areas were assessed by confocal micro-Raman spectroscopy showing that at low laser fluences the polymer structure remained almost unaltered. In addition, Raman spectra of hydrated samples recovered the original shape of areas structured at low laser fluence.

Keywords: DLIP; laser materials processing; diffraction gratings; ophthalmic materials; polymers



Citation: Sola, D.; Milles, S.; Lasagni, A.F. Direct Laser Interference Patterning of Diffraction Gratings in Safrofilcon-A Hydrogel: Fabrication and Hydration Assessment. *Polymers* **2021**, *13*, 679. <https://doi.org/10.3390/polym13050679>

Academic Editor: Jem-Kun Chen

Received: 1 February 2021

Accepted: 22 February 2021

Published: 24 February 2021

Publisher's Note: MDPI stays neutral with regard to jurisdictional claims in published maps and institutional affiliations.



Copyright: © 2021 by the authors. Licensee MDPI, Basel, Switzerland. This article is an open access article distributed under the terms and conditions of the Creative Commons Attribution (CC BY) license (<https://creativecommons.org/licenses/by/4.0/>).

1. Introduction

Polymer technology has rapidly advanced since the beginning of this century. This development has provided polymers with excellent properties, such as high optical transparency in the UV-visible-NIR spectral region, elasticity, flexibility, durability [1–4], oxygen permeability, hydrophobicity, biostability, and biocompatibility [5–8]. In addition, manufacturing process is easy, reliable, and highly efficient. Polymers are currently the preferred materials in almost all biotechnological applications. In particular, in biomedicine, they have been applied in cardiovascular devices [6], drug delivery [7], as hard and soft tissue replacement [8], and as both contact and intraocular lenses [8–10].

Short and ultrashort pulsed laser radiation has been recently used to structure polymers, crystals, and glasses in applications such as 2D/3D micro/nanostructures [11,12], active and passive waveguides [13–18], photonic crystals [19,20], beam splitters [11,19], data storage elements [11,19,21], and microfluidic components [19,22,23]. In addition, in ophthalmology, ultrashort direct laser writing (UDLW) has been applied to vision correction in photo-refractive surgery [24–26], and more recently, to change the power of refractive optical elements [27–34]. It is well known that diffractive optical elements, such as diffraction gratings, can be used to modify the refractive index and hence the refractive power of an optical device. Specifically, ultrashort laser radiation with laser pulse energy

below damage threshold has been employed to fabricate diffraction gratings within dye-doped and non-doped ophthalmic polymers, resulting in refractive index modification ranging from $\sim 6 \times 10^{-2}$ to $\sim 8 \times 10^{-2}$ [27–34]. Nonetheless, the processing rates reported to date to structure areas of large dimensions, such as the cornea, are low, which hinders their application on a real scale. This limitation can be overcome if the whole pattern, instead of line by line, is transferred to the sample at once. This can be achieved using direct laser interference patterning (DLIP). We have recently proposed DLIP as a novel approach to fabricate diffraction gratings on the surface of ophthalmic polymers to be used for refractive correction [35–37]. DLIP is a single-step and non-contact laser processing technique, which is more flexible and cost-effective when compared to traditional structuring techniques in the micro- and sub-micrometer range [37–42]. To date, we have achieved refractive index changes one order of magnitude higher, with processing yields more than two orders of magnitude faster, than those reported so far by UDLW in similar non-doped ophthalmic polymers [35–37].

Ophthalmic polymers for soft contact lenses are commonly machined in dry stage by lathe cutting to provide them with the required refractive power. Next, they are hydrated by immersion in saline solution for 24 h, providing them the suitable flexibility to be placed over the corneal epithelium. To date, our investigations on DLIP structuring in ophthalmic polymers have been carried out in the dry stage. Nevertheless, accounting for the fact that the final sample is softened by hydration, it is important to assess to what extent the laser structuring modifies the capability of the hydrogel to be hydrated. This evaluation will provide the limiting laser processing parameters to modify the refractive index.

In this work, we investigate how wettability and consequently the hydration process of the polymer sample may be affected by the laser-induced surface patterning. For this purpose, periodic patterns are fabricated by means of DLIP under two-beam configuration with a pulsed laser emitting at 263 nm, and pulsewidth in the nanosecond range. Confocal microscopy and micro-Raman spectroscopy are performed to investigate surface topography, and compositional and structural changes in the laser-processed areas. Finally, static water contact angle (WCA) measurements are carried out with deionized water droplets on the structured areas to evaluate the hydration properties of DLIP structures.

2. Experimental System

2.1. Laser Setup

As the laser source, a Q-Switched Nd:YAG laser emitting at 263 nm with pulsewidth of 4 ns and repetition rate of 1 kHz was used to fabricate the periodic structures (Laser-export Co. Ltd., Tech-263 Advanced, Moscow, Russia). Laser beam was split into two beams of equal intensity by using a diffractive optical element (DOE), and both laser beams were collimated by means of a prism. An optical lens of 60 mm focal length was used to interfere both laser beams on the surface of the sample, as shown in Figure 1. Angle between the laser beams, 2α , and the wavelength of the laser radiation, λ , allowed one to control the interference period, Λ , according to the following equation [38]:

$$\Lambda = \frac{\lambda}{2\sin\alpha}, \quad (1)$$

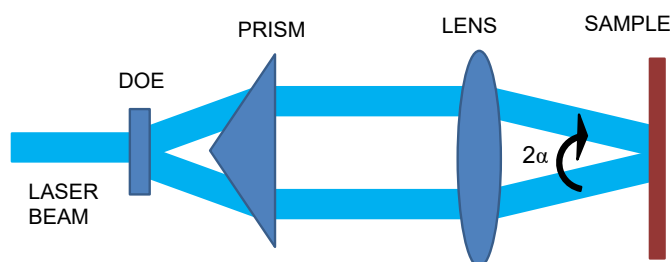


Figure 1. Schematic representation of direct laser interference patterning (DLIP) setup.

Interference spatial periods were experimentally set at 3 μm and 6 μm . Laser fluence was set at 0.47 J/cm², and number of pulses was modified between 2 and 10 pulses. These values were selected after previous experiments to be above the modification threshold and not to induce an excessive damage on the samples.

2.2. Materials

As the substrate, 1 mm thick Safrofilcon-A hydrogel polymer disks, provided by the manufacturer (Contamac Ltd., Saffron Walden, UK) in dry stage, were used to be processed. The optical transmission spectrum is shown in Figure 2.

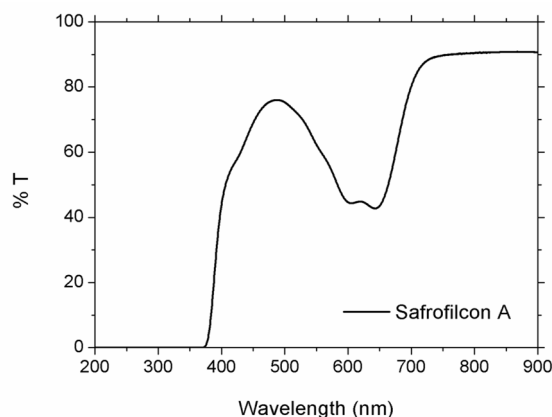


Figure 2. Optical transmission spectra of Safrofilcon-A hydrogel polymer.

2.3. Characterization Techniques

Optical transmission spectra were obtained by means of a spectrophotometer (U-3400, Hitachi, Abingdon, UK). Optical confocal microscopy (Sensofar S Neox, Terrassa, Spain) was performed to investigate surface topographies and height profiles of the structured samples by using a 150 \times microscope objective, which provided an optical resolution of 140 nm and a lateral resolution of 1 nm. Surface roughness was determined by using the arithmetical mean height of the surface, Sa. Confocal micro-Raman spectroscopy was utilized to characterize the microstructural changes using a confocal optical microscope coupled to a spectrometer (SR303i-B, Andor, Belfast, Northern Ireland), equipped with a thermoelectric-cooled CCD detector (Newton 920, Andor, Belfast, Northern Ireland). A continuous wave 785 nm laser was used as the excitation source. Laser power was kept below 50 mW to avoid the heating of the sample. The backscattered light was collected through a 60 \times (0.85 NA) microscope objective lens. Finally, static water contact angle (WCA) measurements were performed using a drop shape analyzer (Krüss DSA 100 S, Hamburg, Germany) and a tensile droplet volume of 2 μL at ambient conditions of 22 $^{\circ}\text{C}$ and 16% of relative humidity. The tangent droplet fitting method was used for all measurements to determine the contact angles between the surface and the droplet. Each measurement was repeated three times for a statistical purpose.

3. Results and Discussion

3.1. DLIP Structuring

The polymer samples were structured with periodic line-like patterns adjusting the experimental setup according to equation 1 to induce spatial periods of 3 μm and 6 μm on the surface of the sample. Multi-pulse laser structuring was carried out delivering 2, 4, 6, 8, and 10 laser pulses at a laser fluence of 0.47 J/cm². Previous experiments allowed one to determine this laser fluence as optimal to process this material. Lower and higher laser fluences were found to be unsuitable since neither produced any effect on the material nor induced significant damage. Figure 3 shows surface topographies of structured samples with spatial periods Λ of 3 μm (a and b) and 6 μm (c and d) using 2 (left) and 6 (right) laser pulses of 0.47 J/cm². Experimental period of the interference pattern was assessed

by confocal microscopy, resulting in $3.03 \pm 0.22 \mu\text{m}$ and $6.10 \pm 0.16 \mu\text{m}$, close to the theoretical values given by Equation (1). It can be observed that the higher the number of pulses, the more material was re-deposited on the surface of the material, thus leading to a more undefined structure. Accounting for the fact that the pulse duration of this laser source was in the nanosecond range, and the high optical absorption of this polymer at the laser wavelength was used to carry out the process (263 nm), the laser intensity was transferred onto the material by both photo-chemical and photo-thermal processes. This type of laser-matter interaction implies direct bond breaking and thermally induced vaporization processes [43].

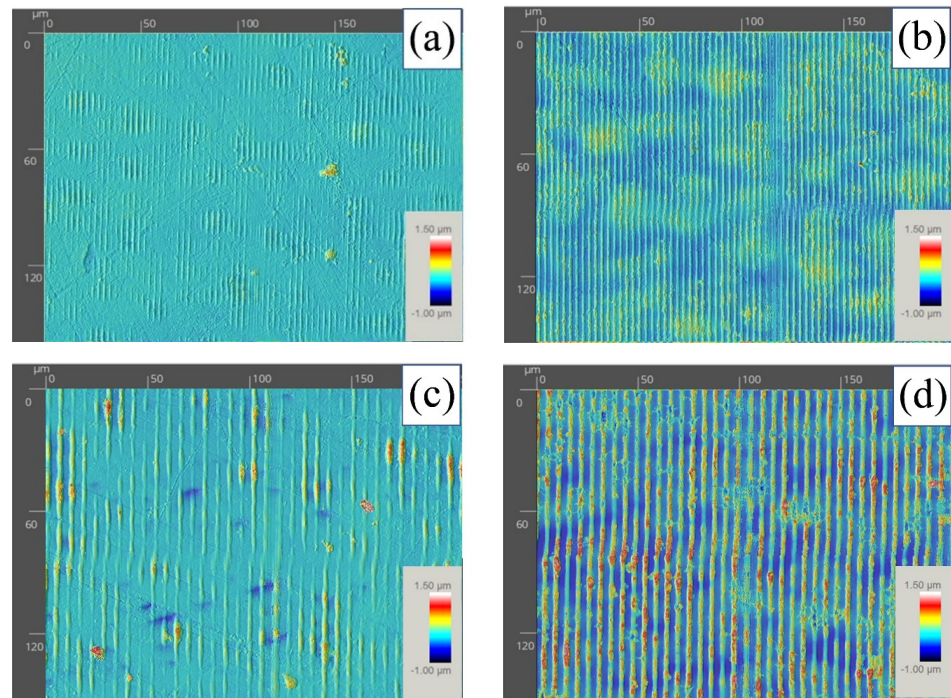


Figure 3. Confocal topographies of structured samples with spatial periods Λ of $3 \mu\text{m}$ (a,b) and $6 \mu\text{m}$ (c,d) using 2 (left) and 6 (right) laser pulses of $0.47 \text{ J}/\text{cm}^2$.

Next, profile measurements were taken by using confocal microscopy to evaluate the height of DLIP structures. As Figure 4 shows, structured height increased with laser fluence. For the case of samples structured with a spatial period of $3 \mu\text{m}$, the increase was found to be linear. Nevertheless, in samples structured with a spatial period of $6 \mu\text{m}$, the maximal height was achieved at a cumulated laser fluence of $2.82 \text{ J}/\text{cm}^2$ (6 laser pulses of $0.47 \text{ J}/\text{cm}^2$). Higher laser fluences led to a lower height due to both an increased damage induced by the laser radiation in the polymer and to the greater amount of material re-deposited onto the surface as a consequence of the laser ablation process. It is worth highlighting that the height of DLIP structures decreased with the spatial period, in good agreement with previous works found in the literature [41]. In addition to the DLIP height, surface roughness (S_a) was assessed by confocal microscopy, shown in Figure 5. It was observed that roughness was relatively high compared to the structure depth, and that increased with laser fluence until reaching a saturation value. This value was around 160 nm and was achieved with six laser pulses for samples structured with a spatial period of $3 \mu\text{m}$, whereas this saturation value was higher and was reached earlier for samples processed with a spatial period of $6 \mu\text{m}$. Specifically, it was found to be around 300 nm and was achieved with 4 laser pulses.

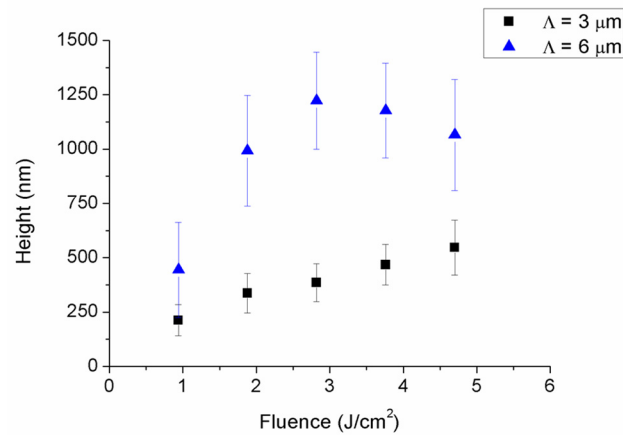


Figure 4. Height of DLIP structures as a function of delivered cumulated laser fluence.

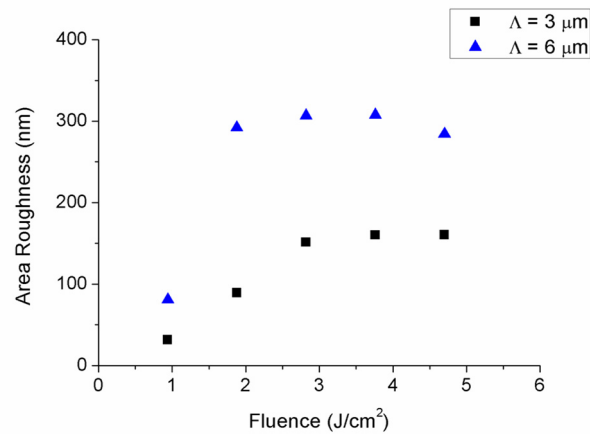


Figure 5. Surface roughness of structured samples as a function of delivered fluence.

3.2. Hydration Assessment

Static water contact angle (WCA) measurements were performed to evaluate the wetting characteristics of the laser-structured areas. Figure 6 shows time-dependent measurements taken during the absorption of the water droplet by the polymer samples. It can be observed that all samples showed the same behavior; departing from the initial WCA value, it decreased as a function of time until an inflection point appeared for a WCA value around 9° . Once this point was reached, the curve became flat. For non-processed samples to reach this inflection point took around 19 min. Concerning DLIP-structured samples, the most significant parameter affecting the hydration process was the spatial period. Provided a spatial period, to reach the inflection point took approximately the same time independently of the laser fluence used to structure the sample, specifically, around 22 min and 24 min for samples structured with spatial periods of $6 \mu\text{m}$ and $3 \mu\text{m}$, respectively. Therefore, it was found that hydration process was modified by the laser-induced DLIP structures so that the smaller the spatial period, the longer the time for the sample to be hydrated. In particular, the delay time was estimated in 15% and 26% for Λ of $6 \mu\text{m}$ and $3 \mu\text{m}$, respectively. In addition, although both non-processed and DLIP-structured samples were shown to be hydrophobic, it was observed that the value of the WCA was also affected by the structuring period. For instance, regarding the initial value of the WCA, in non-processed samples it took values around 114° whereas for DLIP-structured samples it took values around 121° and 129° for Λ of $6 \mu\text{m}$ and $3 \mu\text{m}$, respectively. It was also observed that WCA value was also affected by the laser fluence at which the laser structuring was carried out, so that it was increased with the laser fluence. This increase could reach up to a 7% and a 30% in samples structured with spatial periods of $6 \mu\text{m}$

and 3 μm , respectively, when increasing the cumulated laser fluence from 0.94 J/cm^2 to 2.82 J/cm^2 .

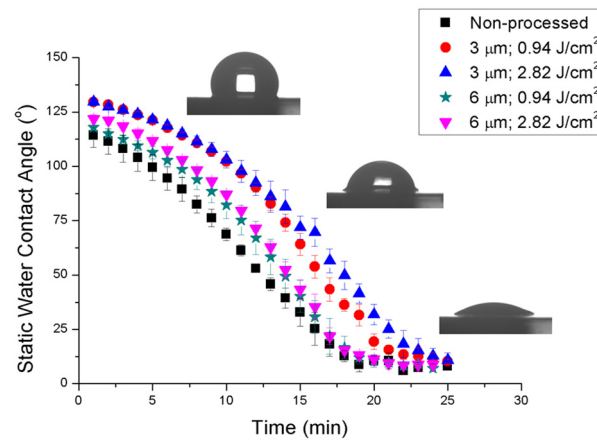


Figure 6. Time-dependent static water contact angle measurements performed during the absorption of the water droplet by the polymer samples.

3.3. Microstructural Characterization

Confocal micro-Raman spectroscopy was performed in laser-structured areas as in dry stage after hydration assessment to investigate modifications in both polymer structure and chemical composition. Figure 7 shows Raman spectra in the wavenumber region $300\text{--}2000 \text{ cm}^{-1}$ of the polymer sample in non-structured regions and in the DLIP processed areas with a spatial period of $3 \mu\text{m}$ at 0.94 J/cm^2 (a) and 2.82 J/cm^2 of cumulated laser fluence (b) before and after hydration assessment. Raman spectra showed sharp peaks and broad bands, which agreed with those previously reported in the literature [44,45]. These peaks and bands were assigned as follows: 605 cm^{-1} , νSCCO ; 646 cm^{-1} , SiO_3 ; 766 cm^{-1} , SiCH_3 ; 1425 cm^{-1} δCH_2 ; 1457 cm^{-1} δCH_2 and δCH_3 ; and 1615 cm^{-1} νCO . It is observed that Raman spectra of areas structured at low cumulated laser fluence, 0.94 J/cm^2 , before and after hydration did not show significant changes when compared with non-processed areas, Figure 7a. Therefore, at low laser fluences the polymer structure remained almost unaltered and hydration process did not produce any substantial modification. However, areas structured at higher fluences showed a strong decrease in the intensity of Raman peaks placed at 646 cm^{-1} , 766 cm^{-1} , 1425 cm^{-1} , 1457 cm^{-1} , and 1615 cm^{-1} , as shown in Figure 7b. This modification resulted from the photo-thermal damaged induced by the laser radiation. It is worth noting that Raman spectra of these samples after hydration process recovered the original shape of areas structured at low laser fluence, as shown in Figure 7b.

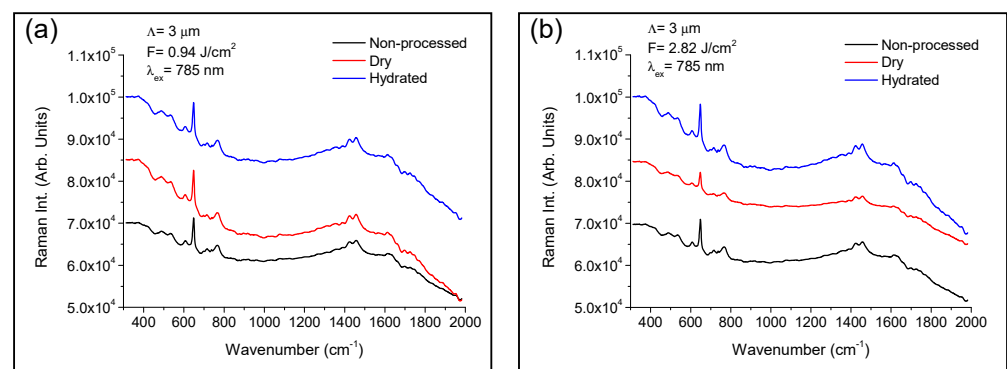


Figure 7. Micro-Raman spectra of the polymer sample in non-processed areas and in the DLIP structured regions with a spatial period of $3 \mu\text{m}$ at 0.94 J/cm^2 laser fluence (a) and 2.82 J/cm^2 laser fluence (b) before and after hydration assessment.

4. Conclusions

Safrofilcon-A hydrogel polymers employed as soft contact lenses were structured on the surface with linear periodic patterns using DLIP with UV pulsed laser radiation in the nanosecond range. The produced periodic patterns were evaluated as a function of the cumulated laser fluence and the spatial period. It was found that height of the DLIP patterns increased with the cumulated laser fluence (or pulse number at a constant fluence). In addition, the height of the periodic structure decreased when the spatial period decreased. Additionally, it was observed that surface roughness increased with both laser fluence and spatial period. Evolution of static water contact angle (WCA) as a function of time was assessed to study how DLIP structures may affect the hydration of the polymer sample. Static water contact angle measurements showed that WCA decreased as a function of time and became flat for a contact angle around 9° . In addition, the laser structured samples induced a delay in the hydration process, so that the shorter the spatial period, the longer the time required for the sample to be hydrated. Delay time was estimated in 15% and 26% for Λ of $6\ \mu\text{m}$ and $3\ \mu\text{m}$, respectively. Contact angle value was affected by the structuring period. It increased for structured samples, so that the larger the spatial period, the lower the contact angle. Micro-Raman analyses carried out in the processed areas showed that at low cumulated laser fluence polymer structure remained almost unaltered. However, high laser fluence induced photo-thermal damaged on the polymer sample. Furthermore, Raman analyses performed after hydration process showed that structured samples recovered the spectra of areas structured at low laser fluence.

Author Contributions: Conceptualization, D.S. and A.F.L.; Investigation, D.S., S.M. Writing—original draft, D.S., S.M., and A.F.L. All authors have read and agreed to the published version of the manuscript.

Funding: This research was funded by European Union's Horizon 2020 research and innovation programme under the Marie Skłodowska-Curie IF No 795630. PIT2 program of the University of Murcia's own research plan and Fundación Séneca grant No 20647/JLI/18 are also acknowledged. The work of A.F. Lasagni is also supported by the German Research Foundation (DFG) under Excellence Initiative program by the German federal and state governments to promote top-level research at German universities.

Institutional Review Board Statement: Not applicable.

Informed Consent Statement: Not applicable.

Data Availability Statement: The data presented in this study are available on request from the corresponding author.

Acknowledgments: Open Access Funding by the Publication Fund of the TU Dresden.

Conflicts of Interest: The authors declare no conflict of interest.

References

1. Rubinstein, M.; Colby, R.H. *Polymer Physics*, 1st ed.; Oxford University Press Inc.: New York, NY, USA, 2003.
2. Schnabel, W. *Polymers and Light*; Wiley: Weinheim, Germany, 2007.
3. Allen, N.S. *Photochemistry and Photophysics of Polymeric Materials*; John Wiley & Sons, Inc.: Hoboken, NJ, USA, 2010.
4. Hussain, F.; Hojjati, M.; Okamoto, M.; Gorga, R.E. Polymer-matrix Nanocomposites, processing, manufacturing, and application: An overview. *J. Compos. Mater.* **2006**, *40*, 1511–1575. [[CrossRef](#)]
5. Scholz, C. *Polymers for Biomedicine: Synthesis, Characterization and Applications*; John Wiley & Sons, Inc.: Hoboken, NJ, USA, 2017.
6. Gupta, S.; Sharma, A.; Verma, R.S. Hydrogel Polymers in biosensor devices for cardiovascular applications. *Curr. Opin. Biomed. Eng.* **2020**, *13*, 69–75. [[CrossRef](#)]
7. Hunter, A.C.; Moghimi, M.S. Smart polymers in drug delivery: A biological perspective. *Polym. Chem.* **2017**, *8*, 41–51. [[CrossRef](#)]
8. Calo, E.; Khutoryanskiy, V.V. Biomedical applications of hydrogels: A review of patents and commercial products. *Eur. Polym. J.* **2015**, *65*, 252–267. [[CrossRef](#)]
9. Maulvi, F.A.; Soni, T.G.; Sha, D.O. A review on therapeutic contact lenses for ocular drug delivery. *Drug Deliv.* **2016**, *23*, 3017–3026. [[CrossRef](#)]
10. Belluchi, R. An introduction to intraocular lenses: Material, optics, haptics, design and aberration. *Cataract* **2013**, *3*, 38–55.
11. Misawa, H.; Juodkazis, S. *3D Laser Microfabrication*; Wiley: Weinheim, Germany, 2006.

12. Sola, D.; Escartin, A.; Cases, R.; Peña, J.I. Crystal growth induced by Nd:YAG laser irradiation in patterning glass ceramic substrates with dots. *Opt. Mater.* **2011**, *33*, 728–734. [[CrossRef](#)]
13. Davis, K.M.; Miura, K.; Sugimoto, N.; Hirao, K. Writing waveguides in glass with a femtosecond laser. *Opt. Lett.* **1996**, *21*, 1729–1731. [[CrossRef](#)] [[PubMed](#)]
14. Sola, D.; Balda, R.; Peña, J.I.; Fernandez, J. Site-selective laser spectroscopy of Nd³⁺ ions in 0.8CaSiO₃-0.2Ca₃(PO₄)₂ biocompatible eutectic glass-ceramics. *Opt. Express* **2012**, *20*, 10701–10711. [[CrossRef](#)] [[PubMed](#)]
15. Sola, D.; de Mendibil, J.M.; de Aldana, J.R.V.; Lifante, G.; Balda, R.; de Aza, A.H.; Pena, P.; Fernandez, J. Stress-induced buried waveguides in the 0.8CaSiO₃-0.2Ca₃(PO₄)₂ eutectic glass doped with Nd³⁺ ions. *Appl. Surf. Sci.* **2013**, *278*, 289–294. [[CrossRef](#)]
16. Chen, F.; Vazquez de Aldana, J.R. Optical waveguides in crystalline dielectric materials produced by femtosecond-laser micromachining. *Laser Photonics Rev.* **2014**, *8*, 251–275. [[CrossRef](#)]
17. de Mendivil, J.M.; Sola, D.; de Aldana, J.R.V.; Lifante, G.; de Aza, A.H.; Pena, P.; Peña, J.I. Ultrafast direct laser writing of cladding waveguides in the 0.8CaSiO₃-0.2Ca₃(PO₄)₂ eutectic glass doped with Nd³⁺ ions. *J. Appl. Phys.* **2015**, *117*, 043104. [[CrossRef](#)]
18. Nolte, S.; Will, M.; Burghoff, J.; Tuennermann, A. Femtosecond waveguide writing: A new avenue to three-dimensional integrated optics. *Appl. Phys. A* **2003**, *77*, 109–111. [[CrossRef](#)]
19. Osellame, R.; Cerullo, G.; Ramponi, R. *Femtosecond Laser Micromachining, Photonic and Microfluidic Devices in Transparent Materials*; Springer: Berlin/Heidelberg, Germany, 2012.
20. Kondo, T.; Matsuo, S.; Juodkasis, S.; Misawa, H. Femtosecond laser interference technique with diffractive beam splitter for fabrication of three-dimensional photonic crystals. *Appl. Phys. Lett.* **2001**, *79*, 725. [[CrossRef](#)]
21. Gamaly, E.G.; Juodkasis, S.; Misawa, H.; Luther-Davies, B.; Rode, A.V.; Hallo, L.; Nicolai, P.; Tikhonchuk, V.T. Formation of nano-voids in transparent dielectrics by femtosecond laser. *Curr. Appl. Phys.* **2008**, *8*, 412–415. [[CrossRef](#)]
22. Cheng, Y.; Sugioka, K.; Midorikawa, K. Microfluidic laser embedded in glass by three-dimensional femtosecond laser microprocessing. *Opt. Lett.* **2004**, *29*, 2007–2009. [[CrossRef](#)]
23. Sugioka, K.; Xu, J.; Wu, D.; Hanada, Y.; Wang, Z.; Cheng, Y.; Midorikawa, K. Femtosecond laser 3D micromachining: A powerful tool for the fabrication of microfluidic, optofluidic, and electrofluidic devices based on glass. *Lab Chip* **2014**, *18*, 3447–3458. [[CrossRef](#)] [[PubMed](#)]
24. McDonald, M.B.; Beuerman, R.; Folzoni, W.; Rivera, L.; Kaufman, H.E. Refractive surgery with the excimer laser. *Am. J. Ophthalmol.* **1987**, *103*, 469. [[CrossRef](#)]
25. Munnerlyn, C.R.; Koons, S.J.; Marschall, J. Photorefractive keratectomy: A technique for laser refractive surgery. *J. Cataract Refract. Surg.* **1988**, *14*, 46–52. [[CrossRef](#)]
26. Pallikaris, I.G.; Papatzanaki, M.E.; Stathi, E.Z.; Frenschock, O.; Georgiadis, A. Laser in situ keratomileusis. *Lasers Surg. Med.* **1990**, *10*, 463–468. [[CrossRef](#)]
27. Ding, L.; Blackwell, R.; Künzler, J.F.; Knox, W.H. Large refractive index change in silicone-based and non-silicone-based hydrogel polymers induced by femtosecond laser micro-machining. *Opt. Express* **2006**, *14*, 11901–11909. [[CrossRef](#)] [[PubMed](#)]
28. Ding, L.; Jani, D.; Linhardt, J.; Künzler, J.F.; Pawar, S.; Labenski, G.; Smith, T.; Knox, W.H. Large enhancement of femtosecond laser micromachining speed in dye-doped hydrogel polymers. *Opt. Express* **2008**, *16*, 21914–21921. [[CrossRef](#)]
29. Ding, L.; Jani, D.; Linhardt, J.; Künzler, J.F.; Pawar, S.; Labenski, G.; Smith, T.; Knox, W.H. Optimization of femtosecond laser micromachining in hydrogel polymers. *J. Opt. Soc. Am.* **2009**, *26*, 1679–1687. [[CrossRef](#)]
30. Xu, L.; Knox, W.H. Lateral gradient index microlenses written in ophthalmic hydrogel polymers by femtosecond laser machining. *Opt. Mater. Express* **2011**, *1*, 1416–1424. [[CrossRef](#)]
31. Huang, R.; Knox, W.H. Femtosecond micro-machining of hydrogels: Parametric study and photochemical model including material saturation. *Opt. Mater. Express* **2019**, *9*, 3818–3834. [[CrossRef](#)]
32. Campaign, S.M.G.; Knox, W.H. Increase in efficacy of near-infrared femtosecond micromachining in ophthalmic hydrogels with the addition of sodium fluorescein, rose bengal, and riboflavin. *Appl. Opt.* **2019**, *58*, 8959–8970. [[CrossRef](#)]
33. Sola, D.; Cases, R. High-repetition-rate femtosecond laser processing of acrylic intra-ocular lenses. *Polymers* **2020**, *12*, 242. [[CrossRef](#)]
34. Sola, D.; de Aldana, J.R.V.; Artal, P. The role of thermal accumulation on the fabrication of diffraction gratings in ophthalmic PHEMA by ultrashort laser direct writing. *Polymers* **2020**, *12*, 2965. [[CrossRef](#)]
35. Sola, D.; Lavieja, C.; Orera, A.; Clemente, M.J. Direct laser interference patterning of ophthalmic polydimethylsiloxane (PDMS) polymers. *Opt. Lasers Eng.* **2018**, *106*, 139–146. [[CrossRef](#)]
36. Sola, D.; Alamri, S.; Lasagni, A.F.; Artal, P. Fabrication and characterization of diffraction gratings in ophthalmic polymers by using UV direct laser interference patterning. *Appl. Surf. Sci.* **2019**, *476*, 128–135. [[CrossRef](#)]
37. Sola, D.; Alamri, S.; Lasagni, A.F. UV Direct Laser Interference Patterning of Diffraction Gratings in Poly-Hydroxyethyl-Methacrylate Ophthalmic Polymers. *J. Laser Micro Nanoeng.* **2020**, *15*, 186–190.
38. Müller-Meskamp, L.; Kim, Y.H.; Roch, T.; Hofmann, S.; Scholz, R.; Eckardt, S.; Leo, K.; Lasagni, A.F. Efficiency enhancement of organic solar cells by fabricating periodic surface textures using direct laser interference patterning. *Adv. Mater.* **2012**, *24*, 906–910. [[CrossRef](#)] [[PubMed](#)]
39. Langheinrich, D.; Yslas, E.; Broglia, M.; Rivarola, V.; Acevedo, D.; Lasagni, A.F. Control of cell growth direction by direct fabrication of periodic micro- and submicrometer arrays on polymers. *J. Polym. Sci. B Polym. Phys.* **2012**, *50*, 415–422. [[CrossRef](#)]

40. Bieda, M.; Siebold, M.; Lasagni, A.F. Fabrication of sub-micron surface structures on copper, stainless steel and titanium using picosecond laser interference patterning. *Appl. Surf. Sci.* **2016**, *387*, 175–182. [[CrossRef](#)]
41. Alamri, S.; Lasagni, A.F. Development of a general model for direct laser interference patterning of polymers. *Opt. Express* **2017**, *25*, 9603–9616. [[CrossRef](#)]
42. Lang, V.; Roch, T.; Lasagni, A.F. High-Speed Surface Structuring of Polycarbonate Using Direct Laser Interference Patterning: Toward $1 \text{ m}^2 \text{ min}^{-1}$ Fabrication Speed Barrier. *Adv. Eng. Mater.* **2016**, *18*, 1342–1348. [[CrossRef](#)]
43. Srinivasan, R.; Braren, B. Ultraviolet laser ablation of organic polymers. *Chem. Rev.* **1989**, *89*, 1303–1316. [[CrossRef](#)]
44. Sekine, Y.; Ikeda-Fukazawa, T. Structural changes of water in a hydrogel during dehydration. *J. Chem. Phys.* **2009**, *130*, 034501. [[CrossRef](#)]
45. Ding, L.; Cancado, L.G.; Novotny, L.; Knox, W.H.; Anderson, N.; Jani, D.; Linhardt, J.; Blackwell, R.I.; Künzler, J.F. Micro-Raman spectroscopy of refractive index microstructures in silicone-based hydrogel polymers created by high-repetition-rate femtosecond laser micromachining. *J. Opt. Soc. Am. B* **2009**, *26*, 595–602. [[CrossRef](#)]